Proceedings of the
47th IEEE Conference on Decision and Control
Cancun, Mexico, Dec. 9-11, 2008



# Formation Tracking Control of Unicycle Teams with Collision Avoidance

Qin Li and Zhong-Ping Jiang

*Abstract*— **In this paper, virtual structure and artificial potential field (APF) based strategies are integrated to realize formation tracking control for a team of unicycles with collision avoidance property. Using virtual structure, each vehicle is required to track a virtual local leader (VLL) for formation maintenance. For inter-vehicle collision avoidance, the motion of each vehicle is restricted in a specified sector area containing the VLL. APF based and backstepping techniques are utilized to design controller that simultaneously satisfy these control objectives.**

## I. INTRODUCTION

Recent years have witnessed the boom of formation control design for multi-vehicle systems due to the needs in many industrial and military applications such as putting out fires, surveillance, search and rescue, and terrain mapping etc.. One of the main problems widely studied is the trajectory tracking or path following with formation, or called formation trajectory tracking or path following problem. For trajectory tracking or path following purpose, one vehicle or some geometric characteristics of the group is required to track the virtual vehicle moving on the given trajectory or to follow the given path. While for formation maintaining, the configuration of the group should be (globally) asymptotically stabilized at some desired geometric pattern, which either is given by the relative positions among the vehicles, or maps to some values (e.g. global or local minimum) of some designed functions (e.g. artificial potential functions). For real applications, there are some extra control objectives which should be achieved. For instances, inter-vehicle and vehicle-obstacle collision avoidances should be guaranteed in the transients of the tracking or path following.

Several types of formation controllers for nonholonomic vehicle teams have been proposed by many researchers during the past a few years. [6], [5], [16], [26], [4], [14], [2] investigate leader-follower structure based strategies, where the vehicle group is layered and each vehicle in some layer has a vehicle in the upper layer as the local leader to follow. And the only vehicle in the top layer is required to track a given trajectory or follow a given path when the group is performing formation tracking or path following task.

APF based approaches have been widely studied for swarming and flocking control of multiple vehicles with holonomic dynamics [19], [22], [27], [20]; and recently been proved useful in reaching some similar purposes for nonholonomic vehicle groups [24], [21], [7], [12], [8]. Using APF based strategy, each vehicle in the group tries to follow the direction specified by the negative gradient of its APF component, and the configuration of the group almost converges to the one that corresponds to local minimum of the collective APF. For holonomic vehicles, this following can be exactly realized at any time; but it may only be achieved in an asymptotical manner for nonholonomic vehicles. The main difficulty of the APF based method is to design an APF without local minima which corresponds to an undesired group configuration.

Another important method for formation control of multi-vehicle systems is based on the virtual structure, which is composed of the reference virtual leaders for the real vehicles to follow. These virtual leaders can be in rigid configurations; interact with each other for some formation control purposes; or interconnect their motions with those of the real vehicles. Early work in this direction can be found in [25], [1]. Recent years have witnessed many efforts in applying this strategy to coordinated tracking and path-following for multi-vehicles with different types of dynamics [11], [9], [15], [13], [8]. See [3] for more work on the topic of formation control.

In this paper, virtual structure and APF based strategies are combined to design a collision-free guaranteed formation tracking controller for a team of unicycles. By adopting virtual structure, the formation tracking problem is translated into that each vehicle in the group is required to track a virtual vehicle (called virtual local leader (VLL), represented by a small circle with number 1-6 in Fig. 1.), which owns pre-given separation and bearing with respect to the one (called virtual formation leader (VFL)) giving the trajectory being tracked. To avoid inter-vehicle collision, the motion of each vehicle is restricted to a pre-specified sector area ($S_i, i = 1, 2, \dots, 6$ in Fig. 1), containing the position of its VLL, whose boundaries are set by different values of the separation and bearing with respect to the VFL. APFs associated with each vehicle is designed such that its unique local minima corresponds to the desired position of the vehicle. And the unboundedness of the APFs at the boundaries of the corresponding sector area prevents each vehicle from leaving it. By using backstepping techniques, a controller is designed to drive each vehicle to follow the negative gradients of its associated APFs in an asymptotical manner. As a result, under some reasonable assumptions on the motion of the VFL, the pose of each vehicle in the group can be shown to converges to that of its VLL asymptotically without colliding with others provided that it is initially located in the corresponding sector.

This work is partly supported by NSF grants ECS-0093176 and DMS-0504462.

Qin Li is with the Department of Electrical and Computer Engineering, Polytechnic University, 6 Metrotech Center, Brooklyn, NY 11201, USA. qli01@students.poly.edu

Zhong-Ping Jiang is with the Department of Electrical and Computer Engineering, Polytechnic University, 6 Metrotech Center, Brooklyn, NY 11201, USA. zjiang@control.poly.edu

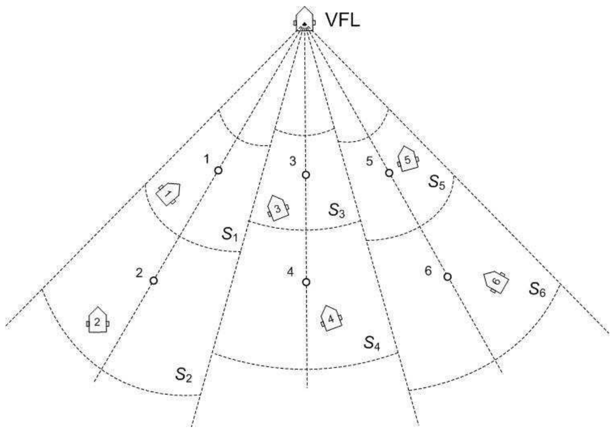


Fig. 1. Illustration of the studied strategy.

The rest of the paper is organized as follows: problem under discussion is formally stated in Section II; Section III is devoted to the controller design procedures; simulations are provided in Section IV; and lastly, concluding remarks will be included in Section V.

## II. Problem Statement

In this work, we consider formation tracking of a team of $N$ unicycles whose dynamics can be described by

$$\begin{aligned} \dot{x}_i &= v_i \cos\phi_i, \\ \dot{y}_i &= v_i \sin\phi_i, \\ \dot{\phi}_i &= \omega_i, \\ \dot{v}_i &= \frac{1}{m_i}F_i, \\ \dot{\omega}_i &= \frac{1}{J_i}\tau_i, \end{aligned} \tag{1}$$

where $(x_i, y_i)$ and $\phi_i$ are respectively the position and orientation of unicycle $i$; and $F_i$ and $\tau_i$ denote the force and torque applied on the vehicle.

The trajectory being tracked by the group is given by the VFL, whose motion is governed by:

$$\begin{aligned} \dot{x}_r &= v_r \cos\phi_r, \\ \dot{y}_r &= v_r \sin\phi_r, \\ \dot{\phi}_r &= \omega_r. \end{aligned} \tag{2}$$

The bearing and separation of vehicle $i$ with respect to the VFL, denoted respectively by $\rho_i$ and $\varphi_i$ (see Fig. 2), evolves as [14]:

$$\dot{\rho}_i = -v_i \cos(\varphi_i - \gamma_i) + v_r \cos\varphi_i, \tag{3}$$
$$\dot{\varphi}_i = -\omega_r + \frac{v_i}{\rho_i}\sin(\varphi_i - \gamma_i) - \frac{v_r}{\rho_i}\sin\varphi_i, \tag{4}$$

where $\gamma_i = \phi_i - \phi_r$ is the difference between the orientations of vehicle $i$ and the VFL. (Note that $\rho_i$ and $\varphi_i$ are center of mass based bearing and separation, which are different with those defined in many works studying leader-follower strategies, e.g. [5], [6], [16], [2] and the references therein.)

By adopting virtual structure strategy, for the formation tracking problem, the position of each vehicle is required to converge to that of its VLL, which has bearing $\rho_i^d$ and separation $\varphi_i^d$ with respect to the VFL (see Fig. 2). Also the body frame of each vehicle is required to track the Serret-Frenet frame attached to the trajectory of the VLL. In addition, considering inter-vehicle collision avoidance issue, vehicle $i$, $i \in V := \{1, 2, \cdots, N\}$, needs to always stay inside a sector area $S_i$, which is specified by the separation interval $(\rho_i^l, \rho_i^u)$ and bearing interval $(\varphi_i^l, \varphi_i^u)$ with respect to the VFL. (See Fig. 2 for an illustration of $S_1$ for vehicle 1.)

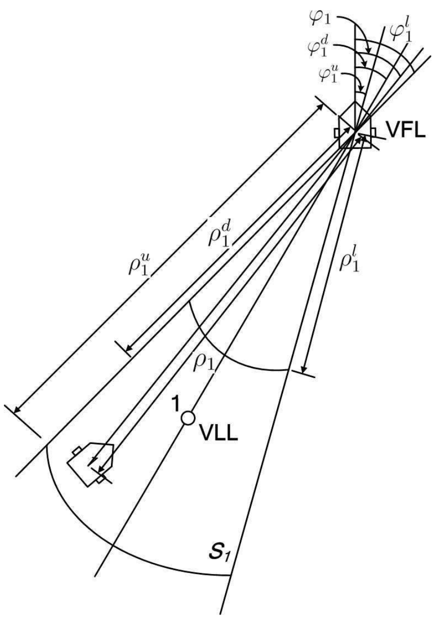


Fig. 2. Illustration of the $\rho - \varphi$ setting.

In this paper, we assume that $\rho_i$, $\varphi_i$ and $\gamma_i$ are known by vehicle $i$, $i \in V$; and $v_r, \omega_r$ and its first and second order derivatives are also available to every vehicle. Thus, the control objectives can be formally stated as: Find $F_i$ and $\tau_i$, $i \in V$, in the forms

$$F_i = F_i(\rho_i, \varphi_i, \gamma_i, v_r, \omega_r, \dot{v}_r, \dot{\omega}_r, \ddot{v}_r, \ddot{\omega}_r),$$
$$\tau_i = \tau_i(\rho_i, \varphi_i, \gamma_i, v_r, \omega_r, \dot{v}_r, \dot{\omega}_r, \ddot{v}_r, \ddot{\omega}_r),$$

such that

$$\lim_{t\to\infty} \rho_i(t) = \rho_i^d, \quad \lim_{t\to\infty} \varphi_i(t) = \varphi_i^d, \tag{5}$$

$$\rho_i(t) \in (\rho_i^l, \rho_i^u), \quad \varphi_i(t) \in (\varphi_i^l, \varphi_i^u), \quad \forall\, t \in [t_0, \infty), \tag{6}$$

$$\lim_{t\to\infty} |\dot{x}_i - \dot{x}_i^d| = 0, \quad \lim_{t\to\infty} |\dot{y}_i - \dot{y}_i^d| = 0, \tag{7}$$

where $\rho_i^l$, $\rho_i^u$, $\varphi_i^u$, $\varphi_i^l$ are constants which satisfy

$$0 < \rho_m < \rho_i^l < \rho_i^u < \rho_M < \infty, \tag{8}$$

$$-\frac{\pi}{2} < -\varphi_M < \varphi_i^l < \varphi_i^u < \varphi_M < \frac{\pi}{2}, \quad \forall\, i \in V, \tag{9}$$

$$\begin{bmatrix} x_i^d \\ y_i^d \end{bmatrix} = \begin{bmatrix} x_r \\ y_r \end{bmatrix} + \begin{bmatrix} \cos\phi_r & -\sin\phi_r \\ \sin\phi_r & \cos\phi_r \end{bmatrix} \begin{bmatrix} -\rho_i^d \cos\varphi_i^d \\ -\rho_i^d \sin\varphi_i^d \end{bmatrix}. \tag{10}$$

## III. Controller Design

Since the controller design procedures are the same for each vehicle, in this section we drop the subscript $i$ in the variables introduced above.

To proceed, we first introduce a type of potential function $V(\cdot, a, b, c) : (a, c) \to [0, +\infty)$, $0 < a < b < c < +\infty$, with the following properties:

1) $V(\cdot, a, b, c) \in C^3(a, c)$;
2) $\frac{\partial V(x,a,b,c)}{\partial x} < 0, \forall x \in (a, b)$; $\frac{\partial V(x,a,b,c)}{\partial x} > 0, \forall x \in (b, c)$;
3) $\lim_{x\to a+} V(x, a, b, c) = \lim_{x\to c-} V(x, a, b, c) = +\infty$;

It is easy to see that the potential function $V(x, a, b, c)$ has a unique minima at $x = b$. Examples of $V$ are

$$V(x,a,b,c) = \begin{cases} A_1 \tan^4\left(\frac{\pi(b-x)}{2(b-a)}\right) + A_2 \quad , \quad x \in (a,b], \\ A_1 \tan^4\left(\frac{\pi(x-b)}{2(c-b)}\right) + A_2 \quad , \quad x \in (b,c), \end{cases} \tag{11}$$

and

$$V(x,a,b,c) = A_3\left(\frac{1}{x-a} + \frac{(c-b)^2}{(b-a)^2}\frac{1}{c-x}\right) + A_4, \quad x \in (a,c), \tag{12}$$

where $A_i, i = 1, 2, 3, 4$ are arbitrary positive real constants.

Next, we define a type of function that plays implemental role in the controller design. Function $g(\cdot, a) : (-\infty, +\infty) \to (-a, +a)$, $0 < a < +\infty$ satisfies:

1) $g(\cdot, a) \in C^2$;
2) $g(0, a) = 0$; $xg(x, a) > 0, \forall x \neq 0$.

An example of such type of function is

$$g(x, a) = 2a/\pi \cdot \arctan(x).$$

In the following, we focus on the design of the control inputs $F$ and $\tau$ using backstepping technique.

*Step 1: Find virtual controls for $v$ and $\gamma$.*

Consider the dynamics of $\rho$ and $\varphi$ in (3) and (4), and, inspired by the work [8], define two virtual inputs $\alpha_v$ and $\alpha_\gamma$ satisfying

$$\alpha_v \cos(\varphi - \alpha_\gamma) = v_r \cos\varphi + K_\rho g_\rho(V'_\rho), \tag{13}$$

$$\alpha_v \sin(\varphi - \alpha_\gamma) = \rho\omega_r + v_r \sin\varphi - \rho g_\varphi(V'_\varphi), \tag{14}$$

where

$$V_\rho(\cdot) := V(\cdot, \rho^l, \rho^d, \rho^u), \ \ V_\varphi(\cdot) := V(\cdot, \varphi^l, \varphi^d, \varphi^u); \tag{15}$$

$$g_\rho(\cdot) := g(\cdot, B_\rho), \ \ g_\varphi(\cdot) := g(\cdot, B_\varphi), \tag{16}$$

with $V'_\rho$ and $V'_\varphi$ denoting $dV_\rho(\rho)/d\rho$ and $dV_\varphi(\varphi)/d\varphi$ respectively; (Later, $V''_\rho$ and $V''_\varphi$ are used to denote respectively $dV^2_\rho(\rho)/d\rho^2$ and $dV^2_\varphi(\varphi)/d\varphi^2$.) $B_\rho$ and $B_\varphi$ are two positive real constants, which will be chosen later; $K_\rho$ may be nonnegative constant or time dependent functions, and also will be selected later.

It can be seen that if $v = \alpha_v$ and $\gamma = \alpha_\gamma$, then we would have

$$\dot\rho = -K_\rho g_\rho(V'_\rho), \quad \dot\varphi = -g_\varphi(V'_\varphi), \tag{17}$$

which will lead to the results of (5) and (6). The main idea of this work is to design control inputs that can realize (17) in asymptotical manner. And Lyapunov based analysis is implemented to guarantee the fulfillment of (5), (6) and (7).

Now, combining (13) and (14), we have

$$\alpha_v \sin\alpha_\gamma = -\rho(\omega_r - g_\varphi(V'_\varphi))\cos\varphi + K_\rho g_\rho(V'_\rho)\sin\varphi, \tag{18}$$

$$\alpha_v \cos\alpha_\gamma = v_r + \rho(\omega_r - g_\varphi(V'_\varphi))\sin\varphi + K_\rho g_\rho(V'_\rho)\cos\varphi. \tag{19}$$

By (18) and (19), we may choose $\alpha_v$ and $\alpha_\gamma$ as

$$\begin{aligned}\alpha_v &= \sqrt{(\alpha_v \sin\alpha_\gamma)^2 + (\alpha_v\cos\alpha_\gamma)^2} \\ &= \Big(\rho^2(\omega_r - g_\varphi(V'_\varphi))^2 + (K_\rho g_\rho(V'_\rho))^2 + v_r^2 + \\ &\quad 2v_r\left(K_\rho g_\rho(V'_\rho)\cos\varphi + \rho(\omega_r - g_\varphi(V'_\varphi))\sin\varphi\right)\Big)^{1/2},\end{aligned} \tag{20}$$

and

$$\begin{aligned}\alpha_\gamma = 2k\pi + \arctan 2\Big(&-\rho(\omega_r - g_\varphi(V'_\varphi))\cos\varphi + \\ &K_\rho g_\rho(V'_\rho)\sin\varphi, v_r + \rho(\omega_r - g_\varphi(V'_\varphi))\sin\varphi \\ &+ K_\rho g_\rho(V'_\rho)\cos\varphi\Big),\end{aligned} \tag{21}$$

where $k \in \mathbb{Z}$. To ensure the continuity and differentiability of $\alpha_v$ and $\alpha_\gamma$, we need to (a) keep $\alpha_v$ away from zero, and (b) let $k$ start at some value, say 0, and vary accordingly (with increment $\pm 1$) whenever $\arctan 2(\alpha_v \sin\alpha_\gamma, \alpha_v\cos\alpha_\gamma)$ has discontinuity, i.e., when $\alpha_v \sin\alpha_\gamma = 0$ and $\alpha_v \cos\alpha_\gamma < 0$.

Now, we address the satisfaction of requirement (a) in different cases.

*Case 1: $v_r$ or $\omega_r$ is uniformly bounded above zero.*

*Assumption 1:* $|\omega_r| > \omega_m > 0$, $\forall t \in [t_0, +\infty)$.

*Assumption 2:* $|v_r| > v_m > 0$, $\forall t \in [t_0, +\infty)$.

*Lemma 1:* Suppose either Assumption 1 or 2 holds; and $\rho$, $\varphi$ satisfies (6), (8) and (9). If $K_\rho = 1$, and $B_\varphi$, $B_\rho$ are selected to satisfy

$$B_\varphi < \omega_m, \tag{22}$$

$$B_\rho < \min\{v_m \cos\varphi_M, \frac{\omega_m - B_\varphi}{\tan\varphi_M}\rho_m\}, \tag{23}$$

then $\alpha_v > 0$ for all $t \geq t_0$.

*Proof:* If Assumption 1 holds, then by (22) and (23), it follows that

$$\left|\frac{\rho(\omega_r - g_\varphi(V'_\varphi))}{K_\rho g_\rho(V'_\rho)}\right| > \frac{\rho_m(\omega_m - B_\varphi)}{B_\rho} > \tan\varphi_M. \tag{24}$$

This shows that $\alpha_v \sin\alpha_\gamma$ cannot be zero, since otherwise we have from (18) that

$$\frac{\rho(\omega_r - g_\varphi(V'_\varphi))}{K_\rho g_\rho(V'_\rho)} = \tan\varphi < \tan\varphi_M. \tag{25}$$

Now, if Assumption 2 holds, we prove that $\alpha_v \sin\alpha_\gamma$ and $\alpha_v \cos\alpha_\gamma$ cannot be both zero. By contradiction, suppose both were zero. Then we have seen that $\alpha_v \sin\alpha_\gamma = 0$ gives

$\rho(\omega_r - g_\varphi(V'_\varphi)) = K_\rho g_\rho(V'_\rho)\tan\varphi$, which combines with (19) shows

$$K_\rho g_\rho(V'_\rho) = -v_r\cos\varphi. \tag{26}$$

But from (23),

$$|K_\rho g_\rho(V'_\rho)| < B_\rho < v_m\cos\varphi_M < |v_r\cos\varphi|. \tag{27}$$

∎

*Case 2: $v_r$ is upper bounded; $v_r$ and $\omega_r$ do not simultaneously vanish.*

*Assumption 3:* $|v_r| < v_M < +\infty$, $\forall t \in [t_0, +\infty)$; for some $\omega_m > 0$, $\{t \in [t_0, +\infty) : v_r(t) = 0, |\omega_r(t)| < \omega_m\} = \emptyset$.

*Lemma 2:* Suppose either Assumption 3 holds; and $\rho$, $\varphi$ satisfies (6), (8) and (9). Then $\alpha_v > 0$ if

$$K_\rho = v_r^2,\ \ B_\rho < \frac{\cos\varphi_M}{v_M},\ \ B_\varphi < \omega_m. \tag{28}$$

*Proof:* By contradiction, suppose $\alpha_v\sin\alpha_\gamma$ and $\alpha_v\cos\alpha_\gamma$ were both zero. It would follow that (25) and (26) hold. But, if $v_r \neq 0$, we have

$$\left|\frac{K_\rho g_\rho(V'_\rho)}{v_r}\right| < v_M B_\rho < \cos\varphi_M \neq \cos\varphi, \tag{29}$$

which contradicts with (26); while if $v_r = 0$, then by the assumption, $|\omega_r| > \omega_m > B_\varphi$, thus

$$\left|\frac{\rho(\omega_r - g_\varphi(V'_\varphi))}{K_\rho g_\rho(V'_\rho)}\right| = \infty, \tag{30}$$

which contradicts with (25). ∎

In the rest of this section, backstepping techniques are used to derive the input force $F$ and torque $\tau$.

*Step 2: Find a virtual control for $\omega$.*

Consider the potential function

$$V_1 = V_\rho + V_\varphi. \tag{31}$$

We have,

$$\begin{aligned}
\dot V_1 &= V'_\rho\cdot\dot\rho + V'_\varphi\cdot\dot\varphi \\
&= V'_\rho(v_r\cos\varphi - v\cos(\varphi-\gamma)) + \\
&\quad V'_\varphi\left(-\omega_r + \frac{v}{\rho}\sin(\varphi-\gamma) - \frac{v_r}{\rho}\sin\varphi\right) \\
&= V'_\rho(-K_\rho g_\rho(V'_\rho) + \alpha_v\cos(\varphi-\alpha_\gamma) - \\
&\quad v\cos(\varphi-\gamma)) + V'_\varphi\Big(-g_\varphi(V'_\varphi) - \\
&\quad \frac{\alpha_v}{\rho}\sin(\varphi-\alpha_\gamma) + \frac{v}{\rho}\sin(\varphi-\gamma)\Big) \\
&= -K_\rho V'_\rho g_\rho(V'_\rho) - V'_\varphi g_\varphi(V'_\varphi) - \\
&\quad V'_\rho\Big(v_e\cos(\varphi-\gamma) + \alpha_v\big((\cos\gamma_e - 1)\cos(\varphi-\alpha_\gamma) \\
&\quad + \sin\gamma_e\sin(\varphi-\alpha_\gamma)\big)\Big) + \frac{V'_\varphi}{\rho}\Big(v_e\sin(\varphi-\gamma) + \\
&\quad \alpha_v\big((\cos\gamma_e - 1)\sin(\varphi-\alpha_\gamma) \\
&\quad - \sin\gamma_e\cos(\varphi-\alpha_\gamma)\big)\Big),
\end{aligned} \tag{32}$$

where

$$v_e = v - \alpha_v, \quad \gamma_e = \gamma - \alpha_\gamma. \tag{33}$$

Now, consider the function

$$V_2 = V_1 + \frac{1}{2}\gamma_e^2. \tag{34}$$

Then we have,

$$\begin{aligned}
\dot V_2 &= -K_\rho V'_\rho g_\rho(V'_\rho) - V'_\varphi g_\varphi(V'_\varphi) + \\
&\quad v_e\left(\frac{1}{\rho}V'_\varphi\sin(\varphi-\gamma) - V'_\rho\cos(\varphi-\gamma)\right) + \\
&\quad \gamma_e\Bigg(\omega - \omega_r - \dot\alpha_\gamma - \alpha_v\cos(\varphi-\alpha_\gamma)\cdot \\
&\quad \left(V'_\rho\frac{\cos\gamma_e - 1}{\gamma_e} + \frac{V'_\varphi}{\rho}\frac{\sin\gamma_e}{\gamma_e}\right) + \alpha_v\sin(\varphi-\alpha_\gamma)\cdot \\
&\quad \left(\frac{V'_\varphi}{\rho}\frac{\cos\gamma_e - 1}{\gamma_e} - V'_\rho\frac{\sin\gamma_e}{\gamma_e}\right)\Bigg),
\end{aligned} \tag{35}$$

where note that

$$\frac{\sin\gamma_e}{\gamma_e} = \int_0^1\cos\xi\gamma_e d\xi, \quad \frac{\cos\gamma_e - 1}{\gamma_e} = -\int_0^1\sin\xi\gamma_e d\xi, \tag{36}$$

are smooth functions for all $\gamma_e \in \mathbb{R}$.

Denote the virtual control for $\omega$ as $\alpha_\omega$, and let

$$\omega_e = \omega - \alpha_\omega. \tag{37}$$

Choose $\alpha_\omega$ as

$$\begin{aligned}
\alpha_\omega &= -\gamma_e + \omega_r + \dot\alpha_\gamma + \alpha_v\cos(\varphi-\alpha_\gamma)\cdot \\
&\quad \left(V'_\rho\frac{\cos\gamma_e - 1}{\gamma_e} + \frac{V'_\varphi}{\rho}\frac{\sin\gamma_e}{\gamma_e}\right) - \alpha_v\sin(\varphi-\alpha_\gamma)\cdot \\
&\quad \left(\frac{V'_\varphi}{\rho}\frac{\cos\gamma_e - 1}{\gamma_e} - V'_\rho\frac{\sin\gamma_e}{\gamma_e}\right)\Bigg),
\end{aligned} \tag{38}$$

where $\dot\alpha_\gamma$ can be calculated from (21) as

$$\begin{aligned}
\dot\alpha_\gamma &= \dot\varphi + \frac{1}{\alpha_v^2}\Bigg(\dot v_r\Big(\rho\big(\omega_r - g_\varphi(V'_\varphi)\big)\cos\varphi - \\
&\quad K_\rho g_\rho(V'_\rho)\sin\varphi\Big) - \dot\varphi v_r\Big(v_r + \rho\big(\omega_r - g_\varphi(V'_\varphi)\big)\cdot \\
&\quad \sin\varphi + K_\rho g_\rho(V'_\rho)\cos\varphi\Big) - \Big(\dot\rho\big(\omega_r - g_\varphi(V'_\varphi)\big) + \\
&\quad \rho\big(\dot\omega_r - g'_\varphi(V'_\varphi)V''_\varphi\dot\varphi\big)\Big)\cdot\Big(v_r\cos\varphi + K_\rho g_\rho(V'_\rho)\Big) \\
&\quad + \Big(\dot K_\rho g_\rho(V'_\rho) + K_\rho g'_\rho(V'_\rho)V''_\rho\dot\rho\Big)\cdot\Big(v_r\sin\varphi + \\
&\quad \rho\big(\omega_r - g_\varphi(V'_\varphi)\big)\Big)\Bigg).
\end{aligned} \tag{39}$$

It follows that,

$$\begin{aligned}
\dot V_2 &= -K_\rho V'_\rho g_\rho(V'_\rho) - V'_\varphi g_\varphi(V'_\varphi) - \gamma_e^2 + \\
&\quad v_e\left(\frac{1}{\rho}V'_\varphi\sin(\varphi-\gamma) - V'_\rho\cos(\varphi-\gamma)\right) + \gamma_e\omega_e
\end{aligned} \tag{40}$$

*Step 2: Find input force $F$ and torque $\tau$*

Consider the Lyapunov function

$$W = V_2 + \frac{1}{2}v_e^2 + \frac{1}{2}\omega_e^2. \tag{41}$$

Clearly, we have

$$\begin{aligned}\dot{W} &= -K_\rho V_\rho' g_\rho(V_\rho') - V_\varphi' g_\varphi(V_\varphi') - \gamma_e^2 + \\ &\quad v_e\bigg(\frac{1}{m}F - \dot{\alpha}_v + \frac{1}{\rho}V_\varphi' \sin(\varphi-\gamma) - \\ &\quad V_\rho' \cos(\varphi-\gamma)\bigg) + \omega_e\bigg(\frac{1}{J}\tau - \dot{\alpha}_\omega + \gamma_e\bigg) \quad (42)\end{aligned}$$

Thus, by choosing

$$\begin{aligned}F &= m\bigg( - v_e + \dot{\alpha}_v - \frac{1}{\rho}V_\varphi' \sin(\varphi-\gamma) + \\ &\quad V_\rho' \cos(\varphi-\gamma)\bigg), \quad (43)\\ \tau &= J(-\omega_e + \dot{\alpha}_\omega - \gamma_e), \quad (44)\end{aligned}$$

it follows that

$$\dot{W} = -K_\rho V_\rho' g_\rho(V_\rho') - V_\varphi' g_\varphi(V_\varphi') - \gamma_e^2 - v_e^2 - \omega_e^2. \quad (45)$$

*Theorem 1:* Suppose $\rho(t_0) \in (\rho^l, \rho^u)$, $\varphi(t_0) \in (\varphi^l, \varphi^u)$; $v_r, \dot{v}_r$ and $\omega_r$ are bounded over $[t_0, +\infty)$. Then, by the inputs given in (43) and (44), the control objectives (5), (6) and (7) can be achieved if we further have either set of the following conditions is satisfied:

i) Assumption 1 or 2 holds, and $K_\rho$, $B_\rho$ and $B_\varphi$ are chosen as in Lemma 1;
ii) Assumption 3 holds; $v_r$ does not converge to zero; and $K_\rho$, $B_\rho$ and $B_\varphi$ are chosen as in Lemma 2.

*Proof:* (sketch) First, from (45) and the property 2) of the function $g$, we know that $\dot{W} \le 0$, for all $t \in [t_0, +\infty)$, which, by the property 3) of the function $V$, can lead to the fact that there exist $\rho^\star$, $\rho_\star \in (\rho^l, \rho^u)$, $\varphi^\star, \varphi_\star \in (\varphi^l, \varphi^u)$ such that

$$\rho(t) \in [\rho_\star, \rho^\star], \quad \varphi(t) \in [\varphi_\star, \varphi^\star], \quad \forall\, t \in [t_0, +\infty]. \quad (46)$$

Next, by Barbalat Lemma [17], we can conclude that the right hand side of (45) converges to zero as $t \to \infty$, which implies

$$\gamma_e \to 0, \quad v_e \to 0, \quad \omega_e \to 0, \quad (47)$$

$$K_\rho V_\rho' g_\rho(V_\rho') \to 0, \quad V_\varphi' g_\varphi(V_\varphi') \to 0, \quad (48)$$

as $t \to +\infty$. From (48) and the continuity of $g$, $V_\varphi'$ and $V_\rho'$, it is not difficult to obtain $\lim_{t\to\infty} \varphi(t) = \varphi^d$, $\lim_{t\to\infty} \rho(t) = \rho^d$.

It remains to prove the result (7). From $\lim_{t\to+\infty} v_e = 0$ and $\lim_{t\to+\infty} \gamma_e = 0$, we have

$$\begin{aligned}\dot{x} &= v\cos\phi = v\cos(\phi_r + \gamma) \to \alpha_v \cos(\phi_r + \alpha_\gamma)\\ &= \cos\phi_r \cdot (\alpha_v \cos\alpha_\gamma) - \sin\phi_r \cdot (\alpha_v \sin\alpha_\gamma), \quad (49)\end{aligned}$$

as $t \to +\infty$. By noting (18), (19), and that $\lim_{t\to+\infty} \rho = \rho^d$, $\lim_{t\to+\infty} \varphi = \varphi^d$, we further reach

$$\begin{aligned}\dot{x} &\to \cos\phi_r(v_r + \rho^d \omega_r \sin\varphi^d) - \sin\phi_r(-\rho^d \omega_r \cos\varphi^d)\\ &= v_r\cos\phi_r + \rho^d\omega_r \sin(\phi_r + \varphi^d) = \dot{x}^d, \quad (50)\end{aligned}$$

as $t \to +\infty$. The convergence of $\dot{y}$ can be shown similarly, hence omitted. ∎

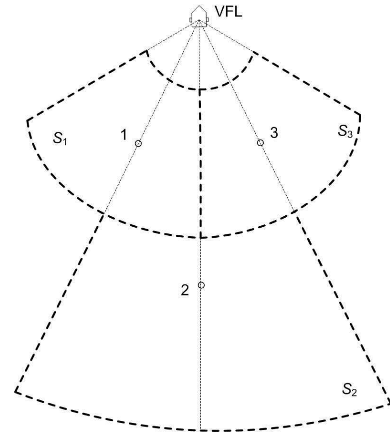


Fig. 3. The safety sectors and desired formation in the simulation.

## IV. SIMULATIONS

In this section, we simulate our control law with three unicycles. The parameters of the safety sectors $S_i, i = 1, 2, 3$, and desired formation are listed in the following Table I and also illustrated in Fig. 3:

TABLE I
PARAMETERS OF THE SAFETY SECTORS AND DESIRED FORMATION

| Vehicle No. | Parameters |
|---|---|
| 1 | $\rho_1^d = 5,\ \rho_1^l = 2,\ \rho_1^u = 8,$ $\varphi_1^d = -\frac{\pi}{6},\ \varphi_1^l = -\frac{\pi}{3},\ \varphi_1^u = 0.$ |
| 2 | $\rho_2^d = 10,\ \rho_1^l = 8,\ \rho_1^u = 16,$ $\varphi_2^d = 0,\ \varphi_2^l = -\frac{\pi}{6},\ \varphi_2^u = \frac{\pi}{6}.$ |
| 3 | $\rho_3^d = 5,\ \rho_3^l = 2,\ \rho_3^u = 8,$ $\varphi_3^d = \frac{\pi}{6},\ \varphi_3^l = 0,\ \varphi_3^u = \frac{\pi}{3}.$ |

The initial conditions of the three unicycles are:

TABLE II
INITIAL CONDITIONS OF THE VEHICLE TEAM

| Vehicle No. | Initial Conditions |
|---|---|
| 1 | $\rho_1(t_0) = 4,\ \varphi_1(t_0) = -\frac{\pi}{9},\ \phi_1(t_0) = \frac{2\pi}{3},$ $v_1(t_0) = 0,\ \omega_1(t_0) = 0.$ |
| 2 | $\rho_2(t_0) = 10,\ \varphi_2(t_0) = \frac{\pi}{18},\ \phi_2(t_0) = \pi,$ $v_2(t_0) = 0,\ \omega_2(t_0) = 0.$ |
| 3 | $\rho_3(t_0) = 7,\ \varphi_3(t_0) = \frac{\pi}{18},\ \phi_3(t_0) = \frac{4\pi}{9},$ $v_3(t_0) = 0,\ \omega_3(t_0) = 0.$ |

The function in (12) is used to construct the potential functions $V_\rho$ and $V_\varphi$ with $A_3 = 1$ and $A_4 = 0$. The parameters $B_\rho$ and $B_\varphi$ for, respectively, the functions $g_\rho$ and $g_\varphi$ are picked as 0.5 and 0.2.

We run the simulation in two cases. For both the cases, the VFL is initially posed as $x_r(t_0) = 0, y_r(t_0) = 0, \phi_r(t_0) = \pi/2$. In addition, we have $\dot{v}_r \equiv 0, \dot{\omega}_r \equiv 0,\ \ddot{v}_r \equiv 0, \ddot{\omega}_r \equiv 0$. But, in the first case, we let $v_r(t_0) = 2$ and $\omega_r(t_0) = 0$rad/s; while in the second case, $v_r(t_0)$ and $\omega_r(t_0)$ are initially set to be 2 and 0.15 respectively. The results are plotted in Fig. 4 and 5.

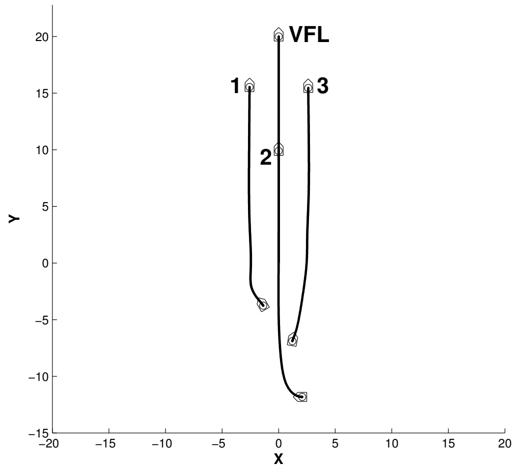


Fig. 4. Simulation with the VFL moving along a straight line: $v_r \equiv 2$, $\omega_r \equiv 0$, $t = 10$s.

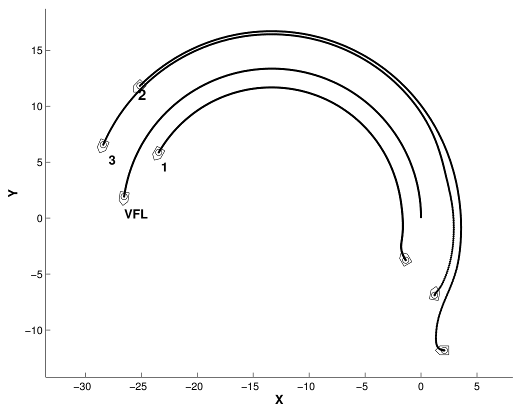


Fig. 5. Simulation with the VFL moving along a circle: $v_r \equiv 2$, $\omega_r \equiv 0.15$, $t = 20$s.

## V. Conclusions

In this paper, by adopting the virtual structure strategy, the formation tracking problem is transformed into the VLL tracking problem for each vehicle. To guarantee the inter-vehicle collision avoidance, APF is designed for each vehicle such that it tends to be unbounded when the vehicle approaches the boundary of a pre-given safety area. Backstepping technique is used to design the control laws that can drive the vehicle to move along the reference path given by the proposed APF, and, consequently, to track the VLL asymptotically.

## References

[1] R. W. Beard, J. Lawton and F. Y. Hadaegh, "A feedback architecture for formation control," *Proc. of American Control Conference*, 2000, pp. 4087-4091.

[2] X. Chen and A. Serrani, "An internal model approach to autonomous leader/follower trailing for non-holonomic vehicles," *International Journal of Robust and Nonlinear Control*, vol. 16, no. 14, 2006, pp. 641-670.

[3] Y. Chen and Z. M. Wang, "Formation control: a review and a new consideration," *Proc. of the IEEE/RSJ International Conference on Intelligent Robots and Systems*, 2005, pp. 3181-3186.

[4] N. Cowan, O. Shakernia, R. Vidal and Shankar Sastry, "Vision-based follow-the-leader," *Proc. of the IEEE/RSJ International Conference on Intelligent Robots and Systems*, 2003, pp. 1796-1801.

[5] A. K. Das, R. Fierro, V. Kumar, J. P. Ostrowski, J. Spletzer and C. J. Taylor, "A vision-based formation control framework," *IEEE Trans. on Robotics and Automation*, vol. 18, no. 5, pp. 813-825, 2002.

[6] J. P. Desai, J. Ostrowski and V. Kumar, "Controlling formations of multiple mobile robots," *Proc. of the IEEE International Conference on Robotics and Automation*, pp. 2864-2869.

[7] D. V. Dimarogonas and K. J. Kyriakopoulos, "On the rendezvous problem for multiple nonholonomic agents," *IEEE Trans. on Automatic Control*, vol. 52, no. 5, 2007. pp. 916-922.

[8] K. D. Do, "Formation tracking control of unicycle-type mobile robots," *Proc. of IEEE Conference on Robotics and Automation*, 2007, pp. 2391-2396.

[9] K. D. Do and J. Pan, "Nonlinear formation control of unicycle-type mobile robots," *Robotics and Autonomous Systems*, vol. 55. pp. 191-204, 2007.

[10] W. J. Dong, Y. Guo and J. A. Farrell, "Formation control of nonholonomic mobile robots," *Proc. of American Control Conference*, 2006, pp. 5602-5607.

[11] M. Egerstedt and X. Hu, "Formation constrained multiagent control," *Proc. of IEEE Conference on Robotics and Automation*, 2001, pp. 3961-3966.

[12] V. Gazi, B. Fidan, Y. S. Hanay and M. I. Köksal, "Aggregation, foraging, and formation control of swarms with non-holonomic agents using potential functions and sliding mode techniques," *Turkey Journal of Electrical Engineering*, vol. 15, no. 2, pp. 149-168, 2007.

[13] R. Ghabcheloo, A. Pascoal, C. Silvestre and I. Kaminer, "Nonlinear coordinated path following control of multiple wheeled robots with bidirectional communication constraints," *International Journal of Adaptive Control and Signal Processing*, vol. 21, pp. 133-157, 2006.

[14] T. Gustavi and X. Hu, "Observer based leader-following formation control using on-board sensor information," *Proc. of Chinese Control Conference*, 2007, pp. 752-755.

[15] I. F. Ihle, M. Arcak and T. I. Fossen, "Passivity-based designs for synchronized path-following," *Automatica*, vol. 43, pp. 1508-1518, 2007.

[16] J. Jongusuk and T. Mita, "Tracking control of multiple mobile robots a case study of inter-robot collision-free problem," *Proc. of the IEEE Int. Conf. on Robotics and Automation*, 2001, pp. 2885-2890.

[17] H. Khalil, *Nonlinear Systems*, 3rd edition. Prentice Hall, 2002.

[18] J. R. T. Lawton, R. W. Beard and B. J. Young, "A decentralized approach to formation maneuvers," *IEEE Trans. on Robotics and Automation,* vol. 19, no. 6, pp. 933-941, 2003.

[19] N. E. Leonard and E. Fiorelli, "Virtual leaders, artificial potentials and coordinated control of groups," *Prof. IEEE Conference on Decision and Control*, 2001, pp. 2968-2973.

[20] Q. Li and Z.-P. Jiang, "Flocking of decentralized multi-agent systems with application to nonholonomic multi-robots," *Proc. of the 17th IFAC World Congress*, 2008, pp. 9344-9349.

[21] S. G. Loizou, D. V. Dimarogonas and K. J. Kyriakopoulos, "Decentralized feedback stabilization of multiple nonholonomic agents," *Proc. of the IEEE Conference on Robotics and Automation*, 2004, pp. 3012-3017.

[22] R. Olfati-Saber, "Flocking for multi-agent dynamic systems: algorithms and theory," *IEEE Trans. on Automatic Control*, vol. 51, no. 3, 2006, pp. 401-420.

[23] O. A. A. Orqueda, X. T. Zhang and R. Fierro, "An output feedback nonlinear decentralized controller for unmanned vehicle coordination," *International Journal of Robust and Nonlinear Control*, vol. 17, no. 12, 2007, pp. 1106-1128.

[24] R. Sepulchre, D. A. Paley, and N. E. Leonard, "Stabilization of planar collective motion with limited communication," *IEEE Trans. on Automatic Control*, accepted.

[25] K. -H. Tan and M. A. Lewis, "Virtual structures for high-precision cooperative mobile robotic control," *Proc. of the IEEE/RSJ International Conference on Intelligent Robots and Systems*, 1996, pp. 132-139.

[26] H. G. Tanner, G. J. Pappas, and V. J. Kumar, "Leader-to-formation stability," *IEEE Trans. on Robotics and Automation*, vol. 20, no. 3, 2004, pp. 443-455.

[27] H. G. Tanner, A. Jadbabaie, and G. J. Pappas, "Flocking in fixed and switching networks," *IEEE Trans. on Automatic Control*, vol. 52, no.5, 2007, pp. 863-868.